Sevoflurane post-conditioning alleviated hypoxic-ischemic brain injury in neonatal rats by inhibiting endoplasmic reticulum stress-mediated autophagy via IRE1 signalings

Jiayuan Niu
Shengjing Hospital of China Medical University
Ziyi Wu
Shengjing Hospital of China Medical University
Hang Xue
Shengjing Hospital of China Medical University
Yahan Zhang
Shengjing Hospital of China Medical University
Qiushi Gao
Shengjing Hospital of China Medical University
Chang Li
Shengjing Hospital of China Medical University
Ping Zhao (zhaoping_sj@163.com)
Shengjing Hospital of China Medical University https://orcid.org/0000-0001-6392-5391

Research Article

Keywords: Sevoflurane post-conditioning, endoplasmic reticulum stress, autophagy, IRE1, hypoxic-ischemic brain injury

Posted Date: April 2nd, 2021

DOI: https://doi.org/10.21203/rs.3.rs-274276/v2

Version of Record: A version of this preprint was published at Neurochemistry International on November 1st, 2021. See the published version at https://doi.org/10.1016/j.neuint.2021.105198.

Abstract

Post-conditioning with sevoflurane, a volatile anesthetic, has been proved to be neuroprotective against hypoxic-ischemic brain injury (HIBI). Our previous research showed that autophagy is over-activated in a neonatal HIBI rat model, and inhibition of autophagy confers neuroprotection. There is increasing recognition that autophagy can be stimulated by activating endoplasmic reticulum (ER) stress. Herein, we purposed to explore: i) the association of ER stress with autophagy in the setting of neonatal HIBI; and ii) the possible roles of ER stress-triggered autophagy, as well as IRE1 signaling in the neuroprotection of sevoflurane post-conditioning against neonatal HIBI. Seven-day-old rats underwent ligation of the left common artery, and a subsequent 2 hour hypoxia (8% O2 / 92% N2). The association of ER stress with autophagy was examined by ER stress inducer (tunicamycin), 4-PBA (ER stress inhibitor), or 3-MA (autophagy inhibitor). Rats in the sevoflurane post-conditioning groups were treated with 2.4% sevoflurane for 30 minutes after HIBI stimulation. The roles of ER stress-mediated autophagy, as well as the IRE1-JNK-beclin1 signaling cascade in the neuroprotection afforded by sevoflurane were explored by ER stress inducer (tunicamycin) and the IRE1 inhibitor (STF-083010). HIBI over-activated ER stress and autophagy in neonatal rats. HIBI-induced autophagy was significantly aggravated by tunicamycin but blocked by 4-PBA; however, HIBI-induced ER stress was not affected by 3-MA. Sevoflurane post-conditioning significantly alleviated ER stress, autophagy, cell apoptosis, and cognitive impairments, which were remarkably abolished by tunicamycin. Also, tunicamycin blocked sevoflurane-induced downregulation of IRE1-JNK-beclin1 signaling pathway. Whereas, IRE1 inhibitor could reverse the effects of tunicamycin. ER stress contributes to autophagy induced by HIBI. Furthermore, sevoflurane post-conditioning significantly protects against HIBI in neonatal rats by inhibiting ER stress-mediated autophagy via IRE1-JNK-beclin1 signaling cascade.

Declarations

Funding

This work was supported by the National Nature Science Foundation of China (No.82071215, No.81870838), Liaoning Province Distinguished Professor Support Program (No. XLYC1802096), Shenyang Clinical Medicine Research Center of Anesthesiology (No. 19-110-4-24, No. 20-204-4-44), and the Outstanding Scientific Fund of Shengjing Hospital (No. 201708).

Conflicts of interest/Competing interests

The authors declare that they have no conflicts of interest.

Availability of data and material

Data will be made available on reasonable request.

Code availability

Not applicable.

Authors' contributions

J.-Y. N. and P. Z. conceived and designed experiments. J.-Y. N., H. X., Q-S. G., Y.-H. Z. and C. L. performed experiments, generated and analyzed the data. Z.-Y. W. wrote the manuscript with the help of P. Z. All authors read and approved the final manuscript.

Ethics approval

Experiments were conducted on Sprague-Dawley rats in accordance with ethical approvals stipulated by the Animal Ethics Committee of Shengjing Hospital, China Medical University, Shenyang, China.

Consent to participate

Not applicable.

Consent for publication

Not applicable.

Introduction

Hypoxic-ischemic brain injury (HIBI) is a specific type of brain injury that result from oxygen deprivation and limited blood flow. HIBI remains among the primary causes of cerebral palsy and other neurodevelopmental disabilities in children, occurring in 1 to 8 per 1000 live births [1]. Although the benefit of therapeutic hypothermia has been shown, over 40% of the cooled infants still die or suffer moderate to severe disabilities [2]. In recent years, the use of medical gases as neuroprotective agents has gained great attention [3]. Sevoflurane is an inhaled anesthetic that is widely used in pediatric medicine and sevoflurane post-conditioning has been proven to protect against cerebral ischemia damage [3]. Therefore, it is critical to explore the benefits of sevoflurane and the underlying molecular mechanisms.

Autophagy is an intracellular self-degradative process involving the elimination of malformed proteins along with damaged organelles via fusing with the lysosome. Our previous study showed that excessive autophagy is involved in cognitive impairments induced by HIBI in neonatal rats [4]. Growing evidence reveal that ER (endoplasmic reticulum) stress cross talks with autophagy [5]. The ER cellular organelle in involved in protein folding along with secretion, biosynthesisof lipids, and calcium homeostasis. Diverse pathophysiologic and pharmacologic insults could disturb proper functioning of the ER; causing aggregation of misfolded, as well as unfolded proteins in the ER, a condition referred to as ER stress [6]. A previous research documented that the compensatory activation of autophagy removes the aggregated dysfunctional proteins emanating from ER stress [7], suggesting that ER stress could constitute a trigger

of autophagy stimulation. Consequently, it is critical to explore the correlation of ER stress with autophagy under neonatal HIBI conditions.

ER stress stimulates an adaptive survival mechanism referred to as the UPR (unfolded protein response), responsible for the recovery of ER homeostasis through attenuation of the translation of proteins, promotion of misfolded protein degradation along with induction of ER-resident chaperones. The UPR constitutes three primary signaling systems activating by three prototypical ER localized stress sensors, i.e., IRE1 (inositol-requiring enzyme-1), ATF6 (activating transcription factor-6), as well as PERK (protein kinase RNA-like endoplasmic reticulum kinase) [8]. During the ER stress, it is speculated that three canonical branches of the UPR in distinctive manners activate autophagy. Particularly, in cells inoculated with JNK (c-Jun N-terminal kinase) inhibitor, or IRE1-deficient cells, the ER stress-triggered autophagy was repressed, demonstrating that the IRE1/JNK cascade is necessary for stimulation of autophagy following ER stress [9]. JNK activation leads to Bcl-2 phosphorylation and dissociation with beclin-1, a well-known key regulator of autophagy [10].

Herein, we assessed the association of ER stress with autophagy in neonatal HIBI rats. Besides, we evaluated the neuroprotective effects of sevoflurane post-conditioning targeting IRE1 signaling cascades between ER stress and autophagy at the molecular level.

Materials And Methods

2.1 Animals

Experiments were conducted on postnatal day 7 (P7) Sprague-Dawley rats as per the guidelines of the Animal Care Committee of Shengjing Hospital, China Medical University, Shenyang, China. Dams along with their pups were put under a cycle of twelve-hour lighting-darkness conditions. Holding facilities were kept at a constant temperature ranging from 21°C to 23°C and the animals free accessed food and water ad libitum. Significant efforts to minimize the number of animals used, as well as any possible suffering were made.

2.2 Experimental design

Experiment I: To evaluate the time course expression of ER stress marker GRP78 and autophagy marker LC3B after HIBI, rat pups (n = 32 per group) were grouped randomly into two groups: Sham group and HI group. The left (ipsilateral) hippocampus was collected from the brains of eight pups randomly selected from every group at each time point (3 hours, 6 hours, 12 hours, and 24 hours after HI) and were prepared for western blot.

Experiment II: To elucidate the association of ER stress with autophagy during HIBI, rat pups (n = 12 per group) were assigned randomly into five groups: Sham, HI, HI + TM (tunicamycin, inducer of ER stress), HI + 4-PBA (sodium 4-phenylbutyrate, inhibitor of ER stress), and HI + 3-MA (3-methyladenine, inhibitor of autophagy). The left (ipsilateral) hippocampus of six pups in all the groups were harvested at 24 h post-

HI for western blot. In addition, we sacrificed six rat pups from every group via transcardiac perfusion with PBS and then 4% PFA for preparation of the brain section at 24 hours after HI.

Experiment III: To evaluate the neuroprotective effects of sevoflurane post-conditioning that target IRE1 signaling cascades between autophagy and ER stress, rat pups (n = 22 per group) were assigned randomly into five groups: Sham, HI, SPC (sevoflurane post-conditioning), SPC + TM, and SPC + TM + IRE1 inhibitor. The left (ipsilateral) hippocampus of six pups in every group were harvested at 24 hours post-HI for western blot. Ten rats in every group were tested in the open field along with the Morris water maze tests at P35 and P35–40, respectively. The other the six rats from every group were used for Nissl stain.

2.3 Neonatal HIBI model, sevoflurane postconditioning, and drug administration

Sevoflurane was employed to anesthetize seven-day-old rats, and subsequently permanent double ligation of the left common carotid artery performed with a 7-0 surgical silk, within five minutes. After waking, we transferred the pups back to cages with their mothers for 2 hours. The pups were then placed in a chamber ventilated with 8% O_2 and 92% N_2 at rate of flow of 2 L/min for 2 hours. Rats in the sevoflurane groups inhaled 2.4% sevoflurane at the rate of flow of 2 L/min for 30 minutes in a chamber under 30% O_2 and 70% N_2 conditions, immediately after HI. Sham control rats were anesthetized and their skin incised and were kept in a chamber under 30% O_2 and 70% N_2 conditions, at the rate of flow of 2 L/min for 2 hours.

The pups received an ICV injection at the left lateral ventricle. Tunicamycin (TM, 25 μM, 5 μL; Sigma-Aldrich, USA), sodium 4-phenylbutyrate (4-PBA, 200 μM, 5 μL; Sigma-Aldrich, USA), 3-methyladenine (3-MA, 10 μM, 5 μL; Proteintech, USA), or IRE1 inhibitor STF-083010 (50μM, 5 μL; MCE, China) was administered into left lateral ventricle 30 minutes prior to HI. The treatment groups' rats that did not receive any drugs received the same volume of 0.1% DMSO alone.

2.4 Western blot analysis

The ipsilateral hippocampus was isolated and kept at -80℃ immediately until use. The RIPA lysis buffer was employed to homogenize the and further span at 14,000 rpm at 4℃ for 30 minutes. We collected the supernatant and then employed the BCA Protein Assay Kit to quantify the proteins. The proteins were then fractionated on a 10% SDS-PAGE gel. After that, the fractionated proteins were blotted onto PVDF membranes. Then, 5% BSA was employed to block the membranes. After that, the membranes were inoculated with the primary antibodies consisting of; anti-GRP78 (1:500, Abcam, UK), anti-LC3B (1:500, Cell Signaling Technology, USA), p62 (1:500, Cell Signaling Technology, USA), IRE-1 (1:500, Abcam, UK), p-IRE-1 (1:500, Abcam, UK), JNK (1:500, Abcam, UK), p-JNK (1:500, Cell Signaling Technology, USA), beclin1 (1:500, Cell Signaling Technology, USA) overnight at 4°C. Thereafter, the membranes were inoculated with specified secondary anti-bodies for 2 hours at room temperature. Immunolabeling was done with the SuperSignal® West Pico Chemiluminescent Substrate (Thermo Scientific, USA). The GE Amersham

Imager 600 was employed to image the immunoblots and the Image J software utilized to analyze the protein bands. β-actin served as the normalization standard.

2.5 TUNEL assay

The in situ Apoptosis Detection Kit (Roche, Switzerland) was employed to perform the TUNEL assay as described by the manufacturer at 24 hours after HI. Briefly, the sections were dewaxed and heated in citrate buffer, followed by inoculation in the blocking buffer (PBS enriched with 10% FBS) for 30 minutes. Next, we inoculated the sections with TdT along with dUTP at 37℃ for 1 hour. DAPI staining of the nuclei was performed. The fluorescence was captured using a Nikon Eclipse NI microscope. The image J software was employed to count the number of TUNEL-positive cells. The data were shown as apoptosis index, quantified as the ratio of (TUNEL-positive cells) / (total cells) × 100%.

2.6 Behavioral tests

The open field test was carried out to assess locomotor and exploratory activities. Each rat was placed at the center of a 100 cm × 100 cm × 50 cm black plastic chamber for minutes. The EthoVision XT software (Noldus, Wageningen, The Netherlands) was employed to record and analyze the tests. After that, 75% alcohol was used to clean the arena after every test to eliminate olfactory cues.

The Morris water maze (MWM) tasks were conducted to explore long-term learning, as well as memory ability. The MWM was composed of a round black pool, with a diameter of 160 cm and depth of 60 cm that was filled with water to a height of 30 cm at room temperature (20 ± 1°C). We placed a cylindrical platform with a diameter of 12-cm into the pool, immersed 1.5 cm deep into the water and 30 cm from the wall. Extra-maze distal cues which had different colors and dimensions were suspended on the black curtains of the pool and were kept constant during the whole experiment. Training sessions took five days and were taken four times a day with an interval of 30 minutes. We placed 10 rats per group into the water to face the pool wall in one of four quadrants. Every rat was allowed 60 seconds to trace the hidden platform. The daily order of entry into these quadrants was randomized. When the escape latency (time used to find the platform) was within 90 seconds, the rats were allowed to remain on the platform for 20 seconds. When the rats could not trace the platform within 90 seconds, we guided them to the platform on which they stayed for 20 seconds and then recorded the escape latency as 90 seconds. In spatial probe task, rats were put into the water and left to swim freely for 90 seconds after removing the platform. An automatic video camera system (Shanghai Mobiledatum Ltd, China) was placed above the pool to record every task.

2.7 Nissl staining

Coronal sections about 3.5 mm from caudal to bregma were harvested for Nissl staining. A digital microscope camera was employed to image the pyramidal cell layer of the CA1 region along with the CA3 region. Microphotographs of cells from three Nissl-stained sections were determined in every rat. Lastly, the image J software was employed to determine the number of healthy, Nissl-positive, neuronal cells.

2.8 Statistical analyses

Statistical analyses were implemented in the GraphPad Prism V.7.0 software. Data are given as mean ± standard deviation (SD). One-way analysis of variance (ANOVA) and subsequent Student–Newman–Keuls post-hoc test were implemented to compare between and within multiple groups. Data for escape latency were compared using two-way repeated measures ANOVA and subsequent Dunnett's multiple comparisons tests. Data for spatial probe test were compared using Dunn's multiple comparison test. P<0.05 signified statistical significance.

Results

3.1 Contents of GRP78 and LC3 increased time dependently post HI

Firstly, ER stress along with autophagy activity in the hippocampus were measured by western blotting at different time points (3hours, 6 hours, 12 hours, and 24 hours) post HI. GRP78 (glucose-regulated protein 78), also referred to as BiP, is a ER resident protein and when under ER stress, it dissociates first from the ER membrane to help destroyed proteins refold and degrade [11]. Stimulation of GRP78 is considered as a biomarker of ER stress [12] and stimulation of autophagy was examined by immunoblotting of LC3B. As indicated in Figure 1, GRP78 expression level was upregulated from 3 h to 24 h post-HI (Figure 1A, B, 3 hours, $p < 0.05$; 6 hours, $p < 0.01$; 12 hours, $p < 0.05$; 24 hours, $p < 0.05$) and the peak GRP78 level was reported at 6 hours after HI. Increase of LC3BII expression started at 6 hours and attained the peak at 24 hours (Figure 1A, C, 6 hours: $p < 0.05$; 12 hours: $p < 0.05$; 24 hours: $p < 0.01$) after HI treatment. Our data illustrated that ER stress along with autophagy participate in the pathological process of neonatal HIBI. Besides, we selected HI-24 hours model for the successive experiments.

3.2 ER stress triggered autophagy in the neonatal HIBI rats

Next, to assess the association of ER stress with autophagy in the context of neonatal HIBI, the rats were inoculated with tunicamycin (ER stress inducer), 4-PBA (ER stress inhibitor), or 3-MA (autophagy inhibitor). The p62 ubiquitin binding protein participates in the selective autophagy and reduction of p62 is a biomarker for increase of autophagic flux [13]. Results showed that HI insult over-activated ER stress and autophagy as indicated by upregulation of GRP78 as illustrated in Figure 2A, B ($p < 0.05$ in contrast with the Sham group) and LC3BII (Figure 2A, C, $p < 0.01$ in contrast with the Sham group), and downregulation of p62 (Figure 2A, D, $p < 0.05$ in contrast with the Sham group). HI-triggered ER stress and autophagy reinforced by combination with TM (Figure 2, GRP78: $p < 0.05$ in contrast with HI group; LC3BII: $p < 0.05$ in contrast with HI group; p62, $p < 0.05$ in contrast with HI group), but counteracted by 4-PBA administration (Figure 2, GRP78: $p < 0.05$ in contrast with HI group; LC3BII: $p < 0.05$ in contrast with HI group; p62, $p < 0.05$ in contrast with HI group). However, 3-MA was able to restrain autophagy activity (Figure 2, LC3BII: $p < 0.05$ in contrast with HI group; p62: $p < 0.05$ in contrast with HI group) without dramatic influences on ER stress (Figure 2, no remarkable difference in GRP78 expression). Altogether, these data illustrated that ER stress occurred upstream of autophagy during neonatal HIBI.

3.3 ER stress-autophagy participates in the cell apoptosis triggered by HIBI

The cell apoptosis in the hippocampus was explored by TUNEL assay. As demonstrated in Figure 3, positive apoptosis cells were seen in HI group (CA1: $p < 0.01$ in contrast with Sham group; CA3: $p < 0.01$ in contrast with Sham group), and treatment with TM enhanced HI-induced apoptosis in the hippocampal CA1and CA3 subregions (CA1: $p < 0.05$ in contrast with HI group; CA3: $p < 0.01$ in contrast with HI group). Interfering ER stress by administration with 4-PBA restrained HI-induced cell apoptosis (CA1: $p < 0.05$ in contrast with HI group; CA3: $p < 0.05$ in contrast with HI group). Similarly, the autophagic inhibitor 3-MA suppressed HI-induced apoptosis via inhibition of autophagy (CA1: $p < 0.05$ in contrast with HI group; CA3: $p < 0.05$ in contrast with HI group).

3.4 Sevoflurane post-conditioning alleviated ER stress-mediated autophagy via regulation of the IRE1 cascade

Our previous researches indicated that sevoflurane-conferred neuroprotection against HIBI is linked to repressed excessive autophagy [14,15]. TM was applied in order to elucidate whether inhibition of autophagy by sevoflurane was mediated through suppressing ER stress. Sevoflurane post-conditioning attenuated HI-induced upregulation in GRP78 and LC3BII, and reduction in p62 (Figure 4A, B, HI in contrast with Sham: $p < 0.05$, $p < 0.01$, $p < 0.01$; SPC in contrast with HI: $p < 0.05$, $p < 0.05$, $p < 0.05$; for GRP78, LC3BII, and p62, respectively), but these effects were blocked by TM (Figure 4A, B, SPC + TM in contrast with SPC: *all p<0.05* for GRP78, LC3BII, and p62, respectively).

Reports document that ER stress can stimulate autophagy through IRE1cascade [16]. The specific IRE1 inhibitor STF-083010 was administrated to further confirm that whether the IRE1-JNK-beclin1 cascade is involved in the neuroprotection of sevoflurane. Proteins in the IRE1 cascade consisting of p-IRE1/IRE1, beclin1, and p-JNK/JNK were also assessed via Western blot. p-IRE1/IRE1, p-JNK/JNK ratio are employed to stand for activation levels of IRE1 and JNK. IRE1 inhibitor reverted the imapcts of TM on the expression of GRP78, LC3BII, and p62 (Figure 4A, B, SPC+TM in contrast with SPC, all $p < 0.05$; SPC+TM+IRE1 inhibitor in contrast with SPC+TM: all $p < 0.05$; for GRP78, LC3BII, and p62, respectively), indicating that sevoflurane restrained ER stress-induced autophagy via the IRE1 cascade during HIBI. As presented in Figure 4, obvious increases in rations of p-IRE1/IRE1, p-JNK/JNK, and expression level of beclin1 were observed in ipsilateral hippocampus of rats in contrast with sham group (Figure 4C, D, HI in contrast with Sham: all $p < 0.05$ for p-IRE1/IRE1, p-JNK/JNK, and beclin1, respectively). Nevertheless, inoculation with sevoflurane dramatically restrained the above changes (Figure 4C, D, SPC in contrast with HI: *all p<0.05* for p-IRE1/IRE1, p-JNK/JNK, and beclin1, respectively), which were reversed by combination with TM (Figure 5, SPC+TM in contrast with SPC: *all p<0.05* for p-IRE1/IRE1, p-JNK/JNK, and beclin1, respectively). IRE1 inhibitor counteracted the effects of TM (Figure 5, SPC+TM+IRE inhibitor in contrast with SPC+TM: *all p<0.05* for p-IRE1/IRE1, p-JNK/JNK, and beclin1, respectively). The above results suggested that sevoflurane post-conditioning suppressed ER stress-autophagy via IRE1-JNK-beclin1 signaling cascade.

3.5 Sevoflurane post-conditioning improved cognitive performance and prevented neuronal loss in rats following HI

To explore the anxiety-like behavior along with the locomotor activity in a novel environment, the rats underwent an open field task at P35. As indicated in Figure 5, no differences were reported among groups in overall travelled distance, time taken in the center region, or the number of feces. These results suggested that treatment factors in this study did not influence anxiety-like behavior or locomotor activity in rats.

From day P35, MWM tasks were carried out to explore spatial learning along with the memory ability. As shown in Figure 5, rats in all groups exhibited a significant downward trend in escape latency. In contrast with the sham group rats, the HI rats exhibited longer escape latency to reach the platform (Figure 5D, day 29 post-HI, $p < 0.05$; day 30 post-HI, $p < 0.001$; day 31 post-HI, $p < 0.001$; day 32 post-HI, $p < 0.001$; day 33 post-HI, $p < 0.001$) and fewer platform crossings (Figure 5E, $p < 0.001$), indicating that rats displayed impaired learning and memory function following HIBI model. Sevoflurane post-conditioning successfully shortened escape latency (Figure 5D, day 30 post-HI, $p < 0.001$; day 31 post-HI, $p < 0.001$; day 32 post-HI, $p < 0.001$; day 33 post-HI, $p < 0.001$) and increased the number of times of crossing the platform (Figure 5E, $p < 0.05$), but these effects were reversed by TM (Figure 5 D, E, escape latency, day 30 post-HI, $p < 0.01$; day 31 post-HI, $p < 0.01$; day 32 post-HI, $p < 0.01$; day 33 post-HI, $p < 0.01$; platform crossing times, $p < 0.05$). However, treatment with IRE1 inhibitor blocked the negative effects of TM (Figure 5 D, E, escape latency, day 31 post-HI, $p < 0.01$; day 32 post-HI, $p < 0.01$; day 33 post-HI, $p < 0.01$; platform crossing times, $p < 0.05$).

Nissl staining procedures were conducted to determine neuron status among groups after behavioral tests. There was an irregular scattered organization of the neurons that had increased intracellular space in the hippocampus of the rats in the HI and SPC +TM groups, whereas neurons in the SPC and SPC + IRE1 inhibitor groups preserved a better functional status. Sevoflurane significantly attenuated HI-induced reduction of neuronal density in the CA1 and CA3 hippocampal areas (HI in contrast with Sham: $p < 0.001$, $p < 0.001$; SPC in contrast with HI: $p < 0.001$, $p < 0.001$; for CA1 and CA3, respectively). Treatment with TM increased neuronal density in the hippocampus (SPC+TM in contrast with SPC: $p < 0.001$, $p < 0.001$ for CA1 and CA3, respectively), while IRE1 inhibitor blocked the effects of TM (SPC+TM+IRE1 inhibitor in contrast with SPC+TM: $p < 0.001$, $p < 0.01$ for CA1 and CA3, respectively).

These results indicated that sevoflurane post-conditioning alleviated HI-induced cognitive impairments, possibly by regulating ER stress-mediated autophagy via IRE1 signaling cascade.

Discussion

HIBI is among the primary causes of neonatal mortality and could cause neurodevelopmental disabilities, with limited therapy options. Excessive autophagy caused by HIBI may cause neuronal death [4]. Our previous studies revealed that the volatile anesthetic sevoflurane could exert neuroprotective effects against HIBI via autophagy inhibition [14,15]. Yet, the underlying mechanisms remain unclear. Herein, we

provided evidence that ER stress contributed to autophagy in HIBI neonatal rats. In addition, sevoflurane post-conditioning alleviated ER stress-dependent autophagy through modulating IRE1-JNK-beclin1 cascades.

Autophagy is among the pathogenetic mechanisms of hypoxic-ischemic cerebral injury [4,17]. Autophagy occurs constitutively at a basal level to sustain cellular homeostasis and function, but can also be triggered by both physiological and pathological stimuli. Previously, we documented that in neonatal rat HIBI model, induction of highly activated autophagy by HI insult it is detrimental and contributes to neuronal apoptosis and cognitive dysfunction [4]. It is emerging increasingly clear that ER stress is one of the signaling cascades involved in regulation of autophagy [18,5]. GRP78 is a central modulator of the ER stress signaling cascade with established function as an ER chaperone protein. During ER stress, it dissociates first from the ER membrane to aid the destroyed proteins to refold and degrade [12]. Thus, activation of GRP78 is considered as a biomarker of ER stress. Herein, both ER stress along with autophagy are activated in the pathological process of neonatal HIBI, as evidenced by increased GRP78 and LC3BII expression, as well as decreased p62 expression. Our results supported results from previous studies that ER stress along with autophagy are involved in ischemic stroke [19,20]. Of note, to elucidate the association of ER stress with autophagy in the setting of neonatal HIBI, the rats were inocualted with TM (ER stress inducer), 4-PBA (ER stress inhibitor), or 3-MA (autophagy inhibitor). Results showed that HIBI-induced autophagy was significantly enhanced by TM but counteracted by 4-PBA; however, HIBI-induced ER stress was not affected by 3-MA. The above data suggested that ER stress is also a prospective inducer of autophagy in neonatal HIBI rats. Similarly, ER stress mediated-autophagy has been implicated in the pathogenesis of traumatic brain injury [21].

Numerous studies have documented that sevoflurane post-conditioning exhibits neuroprotective effects against HIBI, and the protective mechanisms may be attributed to its suppressing autophagy properties. Since ER stress is the upstream cascade inducing autophagy in HIBI, we hypothesized that sevoflurane restrained autophagy through inhibiting ER stress. To confirm this hypothesis, ER stress inductor TM was administrated. Herein, there were remarkable decreases in GRP78 and LC3BII protein levels, whereas increase in p62 protein level following sevoflurane post-conditioning, but these effects were blocked by TM. Alteration of the protein expressions mentioned above revealed that sevoflurane restrained autophagy through inhibiting ER stress.

Our results also suggested that the IRE1-JNK-beclin1 cascade was involved in the mechanisms of neuroprotection of sevoflurane during the inhibition of ER stress-induced autophagy. The UPR is an adaptive cascade that aims to reestablish cellular homeostasis after ER stress. When the UPR occurs, three ER-resident transmembrane proteins (IRE1, ATF6, and PERK) sense it through a luminal domain and transmits to the cytoplasm and nucleus in order to facilitate folding of proteins, attenuation of translation and ER-linked misfolded protein degradation [22]. Interestingly, in a study of IRE1-PERK-ATF6-deficiency in ER stress, autophagy was suppressed in the IRE1 signaling cascade, but not in the PERK and ATF6 cascades [9]. In embryonic fibroblasts, IRE1defect reduced aggregation of LC3-positive vesicles [23]. Under physiological conditions, the ER chaperone GRP78 docks to the regulatory luminal domain of IRE1

and suppresses its activity, whereas in ER stress, GRP78 dissociates from IRE1, allowing it to oligomerize, trans-autophosphorylate, and subsequently activate its endoribonuclease domain [24]. As expected, p-IRE1/IRE1 ratio was increased with HIBI-induced ER stress but decreased by sevoflurane. It has been reported that ER stress-mediated autophagy is modulated via IRE1 cross talk with TRAF2 to induce JNK activation/phosphorylation [9]. Previous investigations have also further illustrated that elevated JNK signaling is linked to autophagy stimulation [25]. One of the key checkpoints in the modulation of autophagy is the interaction between the autophagic effector beclin-1 and the members of the anti-apoptotic Bcl-2 family [26]. Activation of JNK triggered the phosphorylation of Bcl-2 and disrupts the generation of Bcl-2/beclin-1 autophagy repressor complexes [27,28]. Western blot analysis showed that sevoflurane significantly inhibited HI-induced the upregulation of p-IRE1/IRE1, p-JNK/JNK, and beclin-1. TM reversed the effects of sevoflurane on IRE1/JNK/beclin-1 signaling, as well as the autophagy biomarkers LC3B-II and beclin1, and IRE1 inhibitor counteracted the effects of TM. Therefore, the mechanisms by which sevoflurane affects the ER stress-mediated autophagy are attributed to the inhibited of IRE1/JNK/beclin-1 (Figure 7).

In summary, our data have shed some light on the mechanisms of sevoflurane in treatment for HIBI. We established that the ER stress-autophagy signaling is a pivotal mechanistic event that participates in HIBI, and sevoflurane post-conditioning significantly protects against HIBI in neonatal rats by repressing ER stress-mediated autophagy through IRE1-JNK-beclin1 signaling cascade.

References

1. Douglas-Escobar M, Weiss MD (2015) Hypoxic-ischemic encephalopathy: a review for the clinician. JAMA pediatrics 169 (4):397-403. doi:10.1001/jamapediatrics.2014.3269
2. Edwards AD, Brocklehurst P, Gunn AJ, Halliday H, Juszczak E, Levene M, Strohm B, Thoresen M, Whitelaw A, Azzopardi D (2010) Neurological outcomes at 18 months of age after moderate hypothermia for perinatal hypoxic ischaemic encephalopathy: synthesis and meta-analysis of trial data. BMJ (Clinical research ed) 340:c363. doi:10.1136/bmj.c363
3. Wang YZ, Li TT, Cao HL, Yang WC (2019) Recent advances in the neuroprotective effects of medical gases. Medical gas research 9 (2):80-87. doi:10.4103/2045-9912.260649
4. Xu Y, Tian Y, Tian Y, Li X, Zhao P (2016) Autophagy activation involved in hypoxic-ischemic brain injury induces cognitive and memory impairment in neonatal rats. Journal of neurochemistry 139 (5):795-805. doi:10.1111/jnc.13851
5. Qi Z, Chen L (2019) Endoplasmic Reticulum Stress and Autophagy. Advances in experimental medicine and biology 1206:167-177. doi:10.1007/978-981-15-0602-4_8
6. Kaneko M, Imaizumi K, Saito A, Kanemoto S, Asada R, Matsuhisa K, Ohtake Y (2017) ER Stress and Disease: Toward Prevention and Treatment. Biological & pharmaceutical bulletin 40 (9):1337-1343. doi:10.1248/bpb.b17-00342

7. Ding WX, Yin XM (2008) Sorting, recognition and activation of the misfolded protein degradation pathways through macroautophagy and the proteasome. Autophagy 4 (2):141-150. doi:10.4161/auto.5190
8. Lai E, Teodoro T, Volchuk A (2007) Endoplasmic Reticulum Stress: Signaling the Unfolded Protein Response. Physiology 22 (3):193-201. doi:10.1152/physiol.00050.2006
9. Ogata M, Hino S, Saito A, Morikawa K, Kondo S, Kanemoto S, Murakami T, Taniguchi M, Tanii I, Yoshinaga K, Shiosaka S, Hammarback JA, Urano F, Imaizumi K (2006) Autophagy is activated for cell survival after endoplasmic reticulum stress. Molecular and cellular biology 26 (24):9220-9231. doi:10.1128/mcb.01453-06
10. Lorin S, Pierron G, Ryan KM, Codogno P, Djavaheri-Mergny M (2010) Evidence for the interplay between JNK and p53-DRAM signalling pathways in the regulation of autophagy. Autophagy 6 (1):153-154. doi:10.4161/auto.6.1.10537
11. Feng J, Chen Y, Lu B, Sun X, Zhu H, Sun X (2019) Autophagy activated via GRP78 to alleviate endoplasmic reticulum stress for cell survival in blue light-mediated damage of A2E-laden RPEs. BMC Ophthalmology 19 (1):249. doi:10.1186/s12886-019-1261-4
12. Lee AS (2005) The ER chaperone and signaling regulator GRP78/BiP as a monitor of endoplasmic reticulum stress. Methods (San Diego, Calif) 35 (4):373-381. doi:10.1016/j.ymeth.2004.10.010
13. Mathew R, Karp CM, Beaudoin B, Vuong N, Chen G, Chen HY, Bray K, Reddy A, Bhanot G, Gelinas C, Dipaola RS, Karantza-Wadsworth V, White E (2009) Autophagy suppresses tumorigenesis through elimination of p62. Cell 137 (6):1062-1075. doi:10.1016/j.cell.2009.03.048
14. Wang S, Xue H, Xu Y, Niu J, Zhao P (2019) Sevoflurane Postconditioning Inhibits Autophagy Through Activation of the Extracellular Signal-Regulated Kinase Cascade, Alleviating Hypoxic-Ischemic Brain Injury in Neonatal Rats. Neurochemical research 44 (2):347-356. doi:10.1007/s11064-018-2682-9
15. Xue H, Xu Y, Wang S, Wu ZY, Li XY, Zhang YH, Niu JY, Gao QS, Zhao P (2019) Sevoflurane post-conditioning alleviates neonatal rat hypoxic-ischemic cerebral injury via Ezh2-regulated autophagy. Drug design, development and therapy 13:1691-1706. doi:10.2147/dddt.s197325
16. Lee H, Noh J-Y, Oh Y, Kim Y, Chang J-W, Chung C-W, Lee S-T, Kim M, Ryu H, Jung Y-K (2011) IRE1 plays an essential role in ER stress-mediated aggregation of mutant huntingtin via the inhibition of autophagy flux. Human Molecular Genetics 21 (1):101-114. doi:10.1093/hmg/ddr445
17. Lu Q, Harris VA, Kumar S, Mansour HM, Black SM (2015) Autophagy in neonatal hypoxia ischemic brain is associated with oxidative stress. Redox Biology 6:516-523. doi:https://doi.org/10.1016/j.redox.2015.06.016
18. Yorimitsu T, Klionsky DJ (2007) Endoplasmic reticulum stress: a new pathway to induce autophagy. Autophagy 3 (2):160-162. doi:10.4161/auto.3653
19. Chi L, Jiao D, Nan G, Yuan H, Shen J, Gao Y (2019) miR-9-5p attenuates ischemic stroke through targeting ERMP1-mediated endoplasmic reticulum stress. Acta Histochemica 121 (8):151438. doi:https://doi.org/10.1016/j.acthis.2019.08.005

20. Wang P, Shao BZ, Deng Z, Chen S, Yue Z, Miao CY (2018) Autophagy in ischemic stroke. Progress in neurobiology 163-164:98-117. doi:10.1016/j.pneurobio.2018.01.001
21. Wang D-Y, Hong M-Y, Pei J, Gao Y-H, Zheng Y, Xu X (2021) ER stress mediated-autophagy contributes to neurological dysfunction in traumatic brain injury via the ATF6 UPR signaling pathway. Mol Med Rep 23 (4). doi:10.3892/mmr.2021.11886
22. Adams CJ, Kopp MC, Larburu N, Nowak PR, Ali MMU (2019) Structure and Molecular Mechanism of ER Stress Signaling by the Unfolded Protein Response Signal Activator IRE1. Frontiers in Molecular Biosciences 6 (11). doi:10.3389/fmolb.2019.00011
23. Høyer-Hansen M, Jäättelä M (2007) Connecting endoplasmic reticulum stress to autophagy by unfolded protein response and calcium. Cell death and differentiation 14 (9):1576-1582. doi:10.1038/sj.cdd.4402200
24. Pfaffenbach KT, Lee AS (2011) The critical role of GRP78 in physiologic and pathologic stress. Current Opinion in Cell Biology 23 (2):150-156. doi:https://doi.org/10.1016/j.ceb.2010.09.007
25. Zhang Y, Chen P, Hong H, Wang L, Zhou Y, Lang Y (2017) JNK pathway mediates curcumin-induced apoptosis and autophagy in osteosarcoma MG63 cells. Experimental and therapeutic medicine 14 (1):593-599. doi:10.3892/etm.2017.4529
26. Xu HD, Qin ZH (2019) Beclin 1, Bcl-2 and Autophagy. Advances in experimental medicine and biology 1206:109-126. doi:10.1007/978-981-15-0602-4_5
27. He C, Zhu H, Li H, Zou M-H, Xie Z (2013) Dissociation of Bcl-2–Beclin1 Complex by Activated AMPK Enhances Cardiac Autophagy and Protects Against Cardiomyocyte Apoptosis in Diabetes. Diabetes 62 (4):1270-1281. doi:10.2337/db12-0533
28. Wei Y, Pattingre S, Sinha S, Bassik M, Levine B (2008) JNK1-Mediated Phosphorylation of Bcl-2 Regulates Starvation-Induced Autophagy. Molecular Cell 30 (6):678-688. doi:https://doi.org/10.1016/j.molcel.2008.06.001

Figures

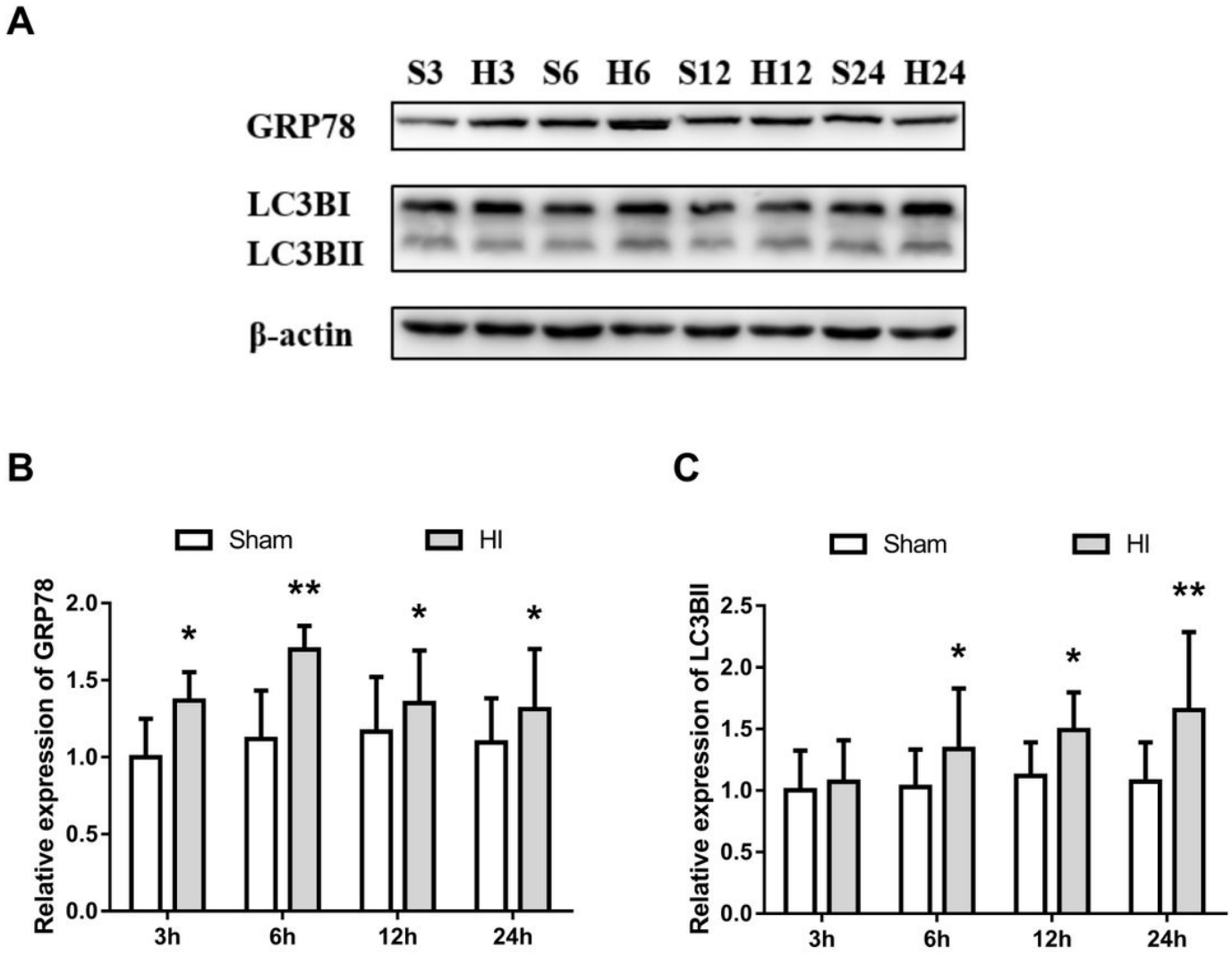

Figure 1

Temporal expression of GRP78 and LC3BII in the ipsilateral hippocampus after HIBI. Levels of GRP78 and LC3BII in the ipsilateral hippocampus were evaluated with Western blot at 3, 6, 12, and 24 h after HI. (A) Representative pictures of Western blotting data. (B) The density of bands analyzed by Image J, with β-actin serving as the normalization control. Data are given as mean ± SD. n = 8 for each group. *$p < 0.05$ and **$p < 0.01$ in contrast with sham group.

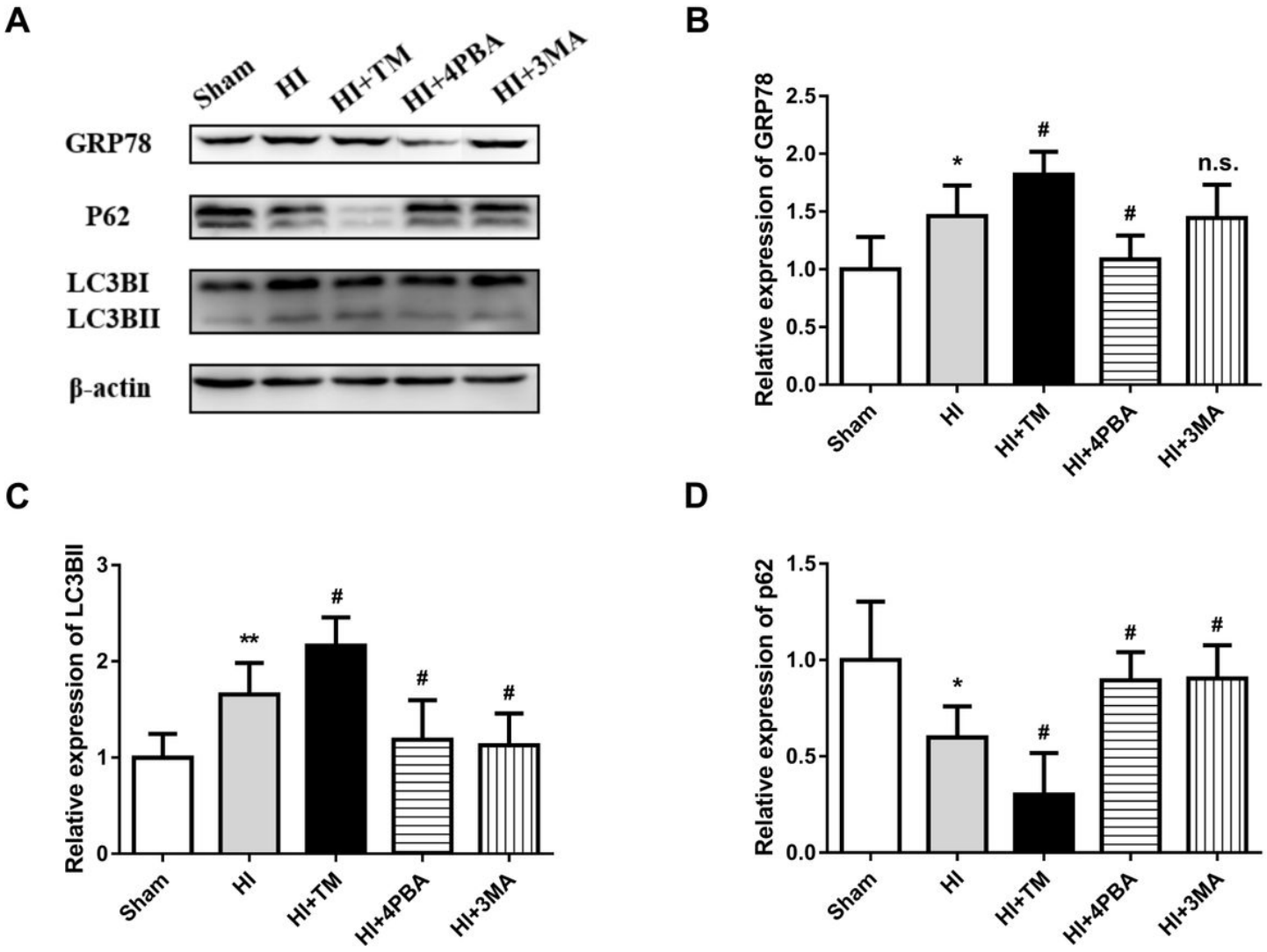

Figure 2

ER stress triggered autophagy in the neonatal HIBI rats. (A) Western blotting data of GRP78, LC3B, and p62. (B) The density of bands analyzed by Image J, with β-actin serving as the normalization control. Data are given as mean ± SD. n = 6 for each group. *p < 0.05 and **p < 0.01 in contrast with Sham group. #p < 0.05 in contrast with HI group.

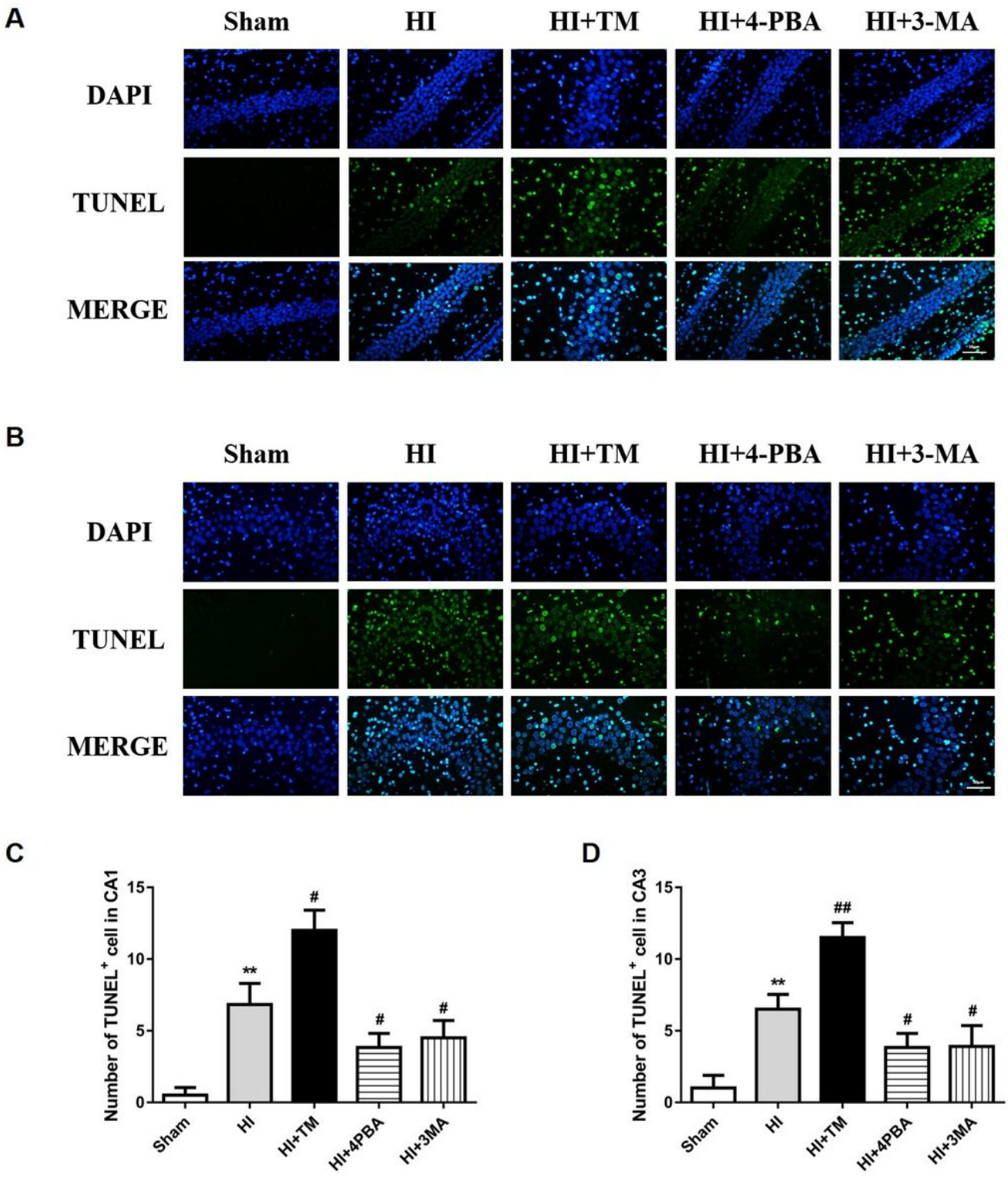

Figure 3

ER stress-autophagy are involved in the cell apoptosis induced by HIBI. (A-B) Images illustrating the TUNEL assay data of apoptosis. Green designates apoptotic cells, while blue designates the nucleus. Scale bar = 50 μm. (C-D) Apoptosis index given as the ratio of (apoptotic cells)/(total cells)×100%. n = 6 for each group. **p < 0.01 in contrast with Sham group. #p < 0.05 and ##p < 0.01 in contrast with HI group.

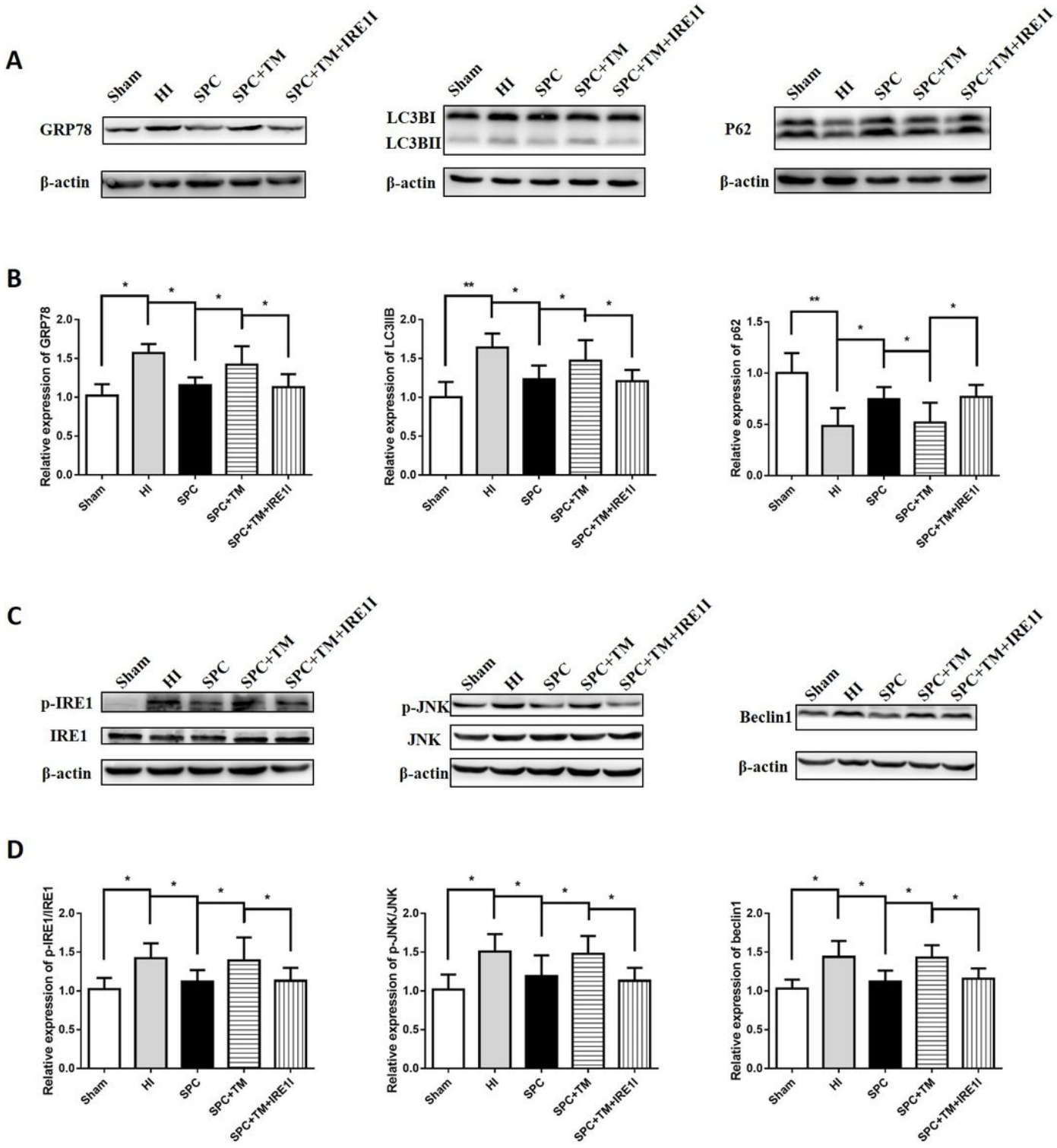

Figure 4

Sevoflurane post-conditioning suppressed ER stress-dependent autophagy via regulating IRE1 cascade. (A) Representative Western blot results of GRP78, LC3B, and p62. (B) The density of bands analyzed by Image J, with β-actin serving as the normalization control. (C) Western blotting data of p-IRE1/IRE1, p-JNK/JNK, and beclin1. (D) The density of bands analyzed by Image J, with β-actin serving as the

normalization control. Data are given as mean ± SD. n = 6 for each group. *p < 0.05 and **p < 0.01 in contrast with the indicated group.

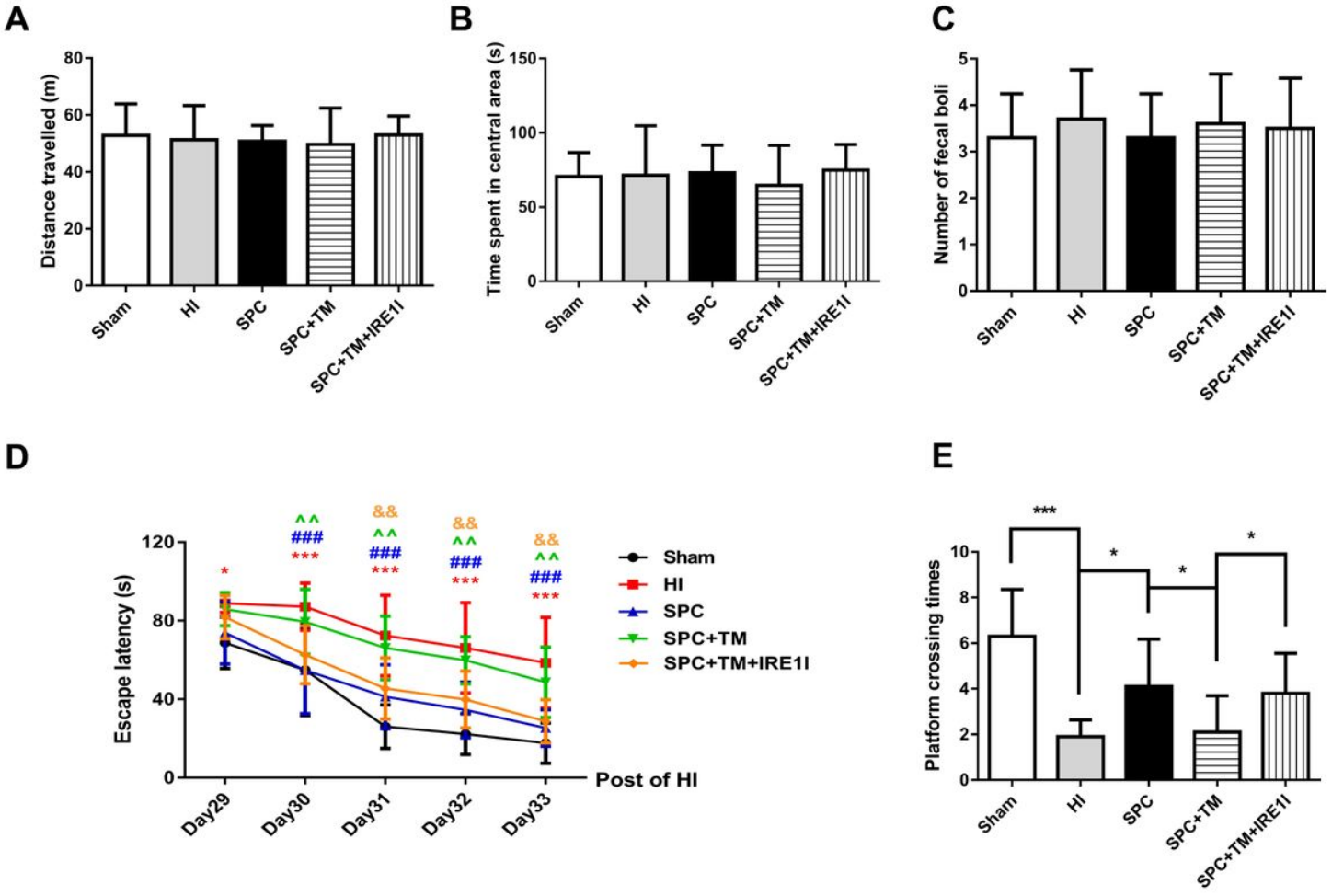

Figure 5

Assessment of the behavior of the rats in the open field test (OFT) and the Morris water maze (MWM) tests in the adolescent phase. (A) Overall travelled distance in the OFT. (B) Time spent in the central area of the OFT. (C) The number of fecal pellets in the OFT. (D) MWM tasks escape latency. (E) Crossing time of the platform in the MWM tasks. Data are given as mean ± SD. n = 10 for each group. In Figure 5D, *p < 0.05 and ***p < 0.001 in contrast with Sham group. ###p < 0.001 in contrast with HI group. ^^p < 0.01 in contrast with SPC group. &&p < 0.01 in contrast with SPC+TM group. In Figure 5E, *p < 0.05 and ***p < 0.001 in contrast with the indicated group.

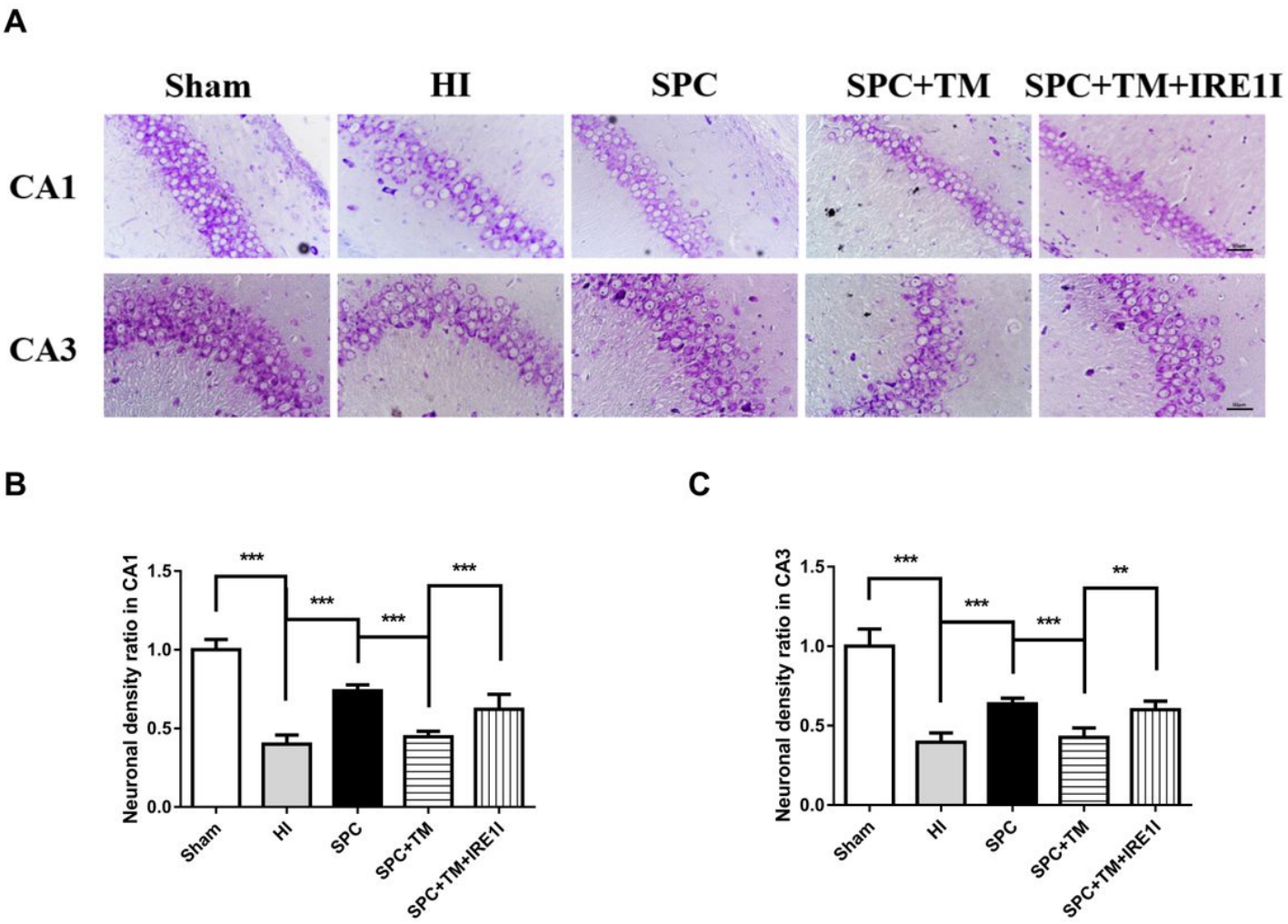

Figure 6

Evaluation of hippocampal neuronal cells in newborn rats with HIBI. (A) Histological Nissl staining in CA1 and CA3 regions of hippocampus. Scale bar = 50μm. (B) Neuronal density ratio in CA1 region of hippocampus. (C) Neuronal density ratio in CA3 region of hippocampus. Data are given as mean ± SD. n = 6 for each group. **p < 0.01 and ***p < 0.001 in contrast with the indicated group.

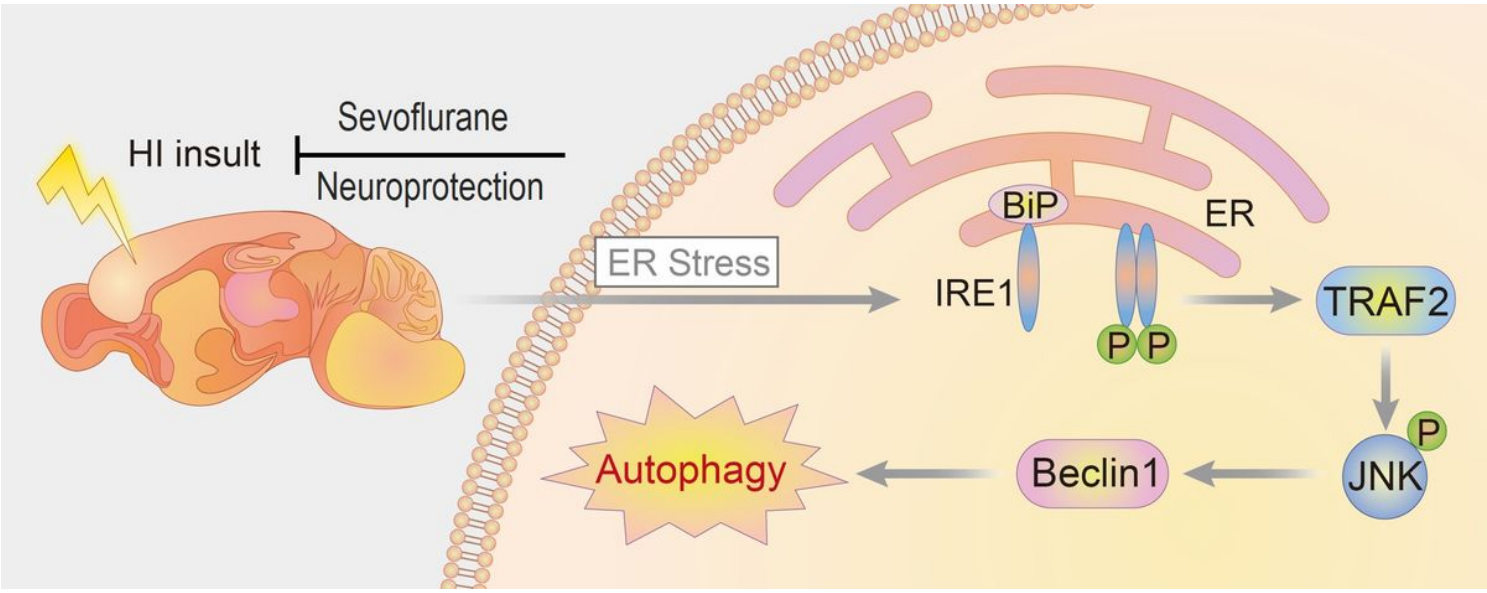

Figure 7

Mechanisms responsible for protective influences of sevoflurane post-conditioning against neonatal hypoxic-ischemic brain injury.